Title	Changes in Neuronal Entropy in a Network Model of the Cortico-Basal Ganglia during Deep Brain Stimulation
Authors(s)	Fleming, John E.; Lowery, Madeleine M.
Publication date	2019-07-27
Conference details	The 2019 41st Annual International Conference of the IEEE Engineering in Medicine and Biology Society (EMBC), Berlin, Germany, 23-27 July 2019
Publisher	IEEE
Item record/more information	http://hdl.handle.net/10197/11280
Publisher's statement	© 2019 IEEE. Personal use of this material is permitted. Permission from IEEE must be obtained for all other uses, in any current or future media, including reprinting/republishing this material for advertising or promotional purposes, creating new collective works, for resale or redistribution to servers or lists, or reuse of any copyrighted component of this work in other works.
Publisher's version (DOI)	10.1109/embc.2019.8857440

Changes in Neuronal Entropy in a Network Model of the Cortico-Basal Ganglia during Deep Brain Stimulation

Author List: John E. Fleming and Madeleine M. Lowery

Author List: John E Fleming and Madeleine M. Lowery

Corresponding Author: Madeleine Lowery

School of Electrical and Electronic Engineering,

University College Dublin, Belfield, Dublin 4, Ireland

madeleine.lowery@ucd.ie

Affiliations: J. E. Fleming and M. M. Lowery are with the School of Electrical and Electronic Engineering, University College Dublin, Ireland.

Link to Published Manuscript, DOI: 10.1109/EMBC.2019.8857440

Details of Funding: Research supported by the European Research Council: ERC-2014-CoG-646923_DBSModel.

Abstract

Neuronal entropy changes are observed in the basal ganglia circuit in Parkinson's disease (PD). These changes are observed in both single unit recordings from globus pallidus (GP) neurons and in local field potential (LFP) recordings from the subthalamic nucleus (STN). These changes are hypothesized as representing changes in the information coding capacity of the network, with PD resulting in a reduction in the coding capacity of the basal ganglia network. Entropy changes in the LFP and in single unit recordings are investigated in a detailed physiological model of the cortico-basal ganglia network during STN deep brain stimulation (DBS). The model incorporates extracellular stimulation of STN afferent fibers, with both orthodromic and antidromic activation, and simulation of the LFP detected at a differential recording electrode. LFP sample entropy and beta-band oscillation power were found to be altered following the application of DBS. The firing pattern entropy of GP neurons in the network were observed to decrease during high frequency stimulation and increase during low frequency stimulation. Simulation results were consistent with experimentally reported changes in neuronal entropy during DBS.

Introduction

Parkinson's disease (PD) is a neurodegenerative disease characterized by a triad of motor symptoms; bradykinesia, akinesia, and tremor. Recent research has focused on identifying signals from the central and peripheral nervous system which can be used to quantify the disease state and symptom severity. These signals are commonly referred to as disease 'biomarkers'. Clinical and experimental studies have identified several potential biomarkers for PD, such as increased oscillatory activity in the beta frequency band (13-30 Hz) recorded from the cortico-basal ganglia circuit [1], betagamma band (60-200 Hz) phase-amplitude coupling in the primary motor cortex [2], and changes in neuronal entropy in the basal ganglia network [3]. Deep brain stimulation is an effective treatment for PD which has been shown to have measurable effects on these biomarkers. These effects include reducing beta-band oscillatory activity [1], reducing betagamma band phase-amplitude coupling [2], and regularizing neural firing rates in the basal ganglia network [4], [5].

Firing pattern entropy, calculated using single unit recordings from the basal ganglia network, and sample entropy, calculated from the STN local field potential (LFP), are two entropy measures with observable changes during PD. Firing pattern entropy quantifies an upper bound on the information embedded in a spike train. Spike trains from globus pallidus (GP) neurons are shown to have increased firing pattern entropy during PD, with this being reduced to near

healthy levels during effective DBS [3]–[6]. Sample entropy is a measure for assessing the complexity of physiological time series signals. In [7], it was shown that there was an inverse relationship between beta-band oscillation power and betaband sample entropy in the STN LFP. Furthermore, in [7] LFP sample entropy was utilized to distinguish between PD patients who experienced freezing of gait episodes and those who did not.

Computational modelling allows the investigation of network dynamics which may be difficult to access during clinical practice. Here a computational model of the corticobasal ganglia network is utilized to investigate changes in basal ganglia neuronal entropy during DBS. Single unit recordings from GP neurons are utilized to assess changes in firing pattern entropy, while the STN LFP is simulated to assess changes in sample entropy and beta-band oscillatory activity during DBS. The results from the computational model are compared with results from clinical and experimental studies. Quantifying changes in basal ganglia entropy may lead to an improved understanding of the relationship between oscillatory activity and entropy in the network, and how this relationship is modified during PD and DBS.

Methods

A physiologically based model of the cortico-basal ganglia network incorporating extracellular DBS and simulation of the STN LFP was utilized [8]. The structure of the network model is presented in Fig. 1 and includes the closed loop formed between the cortex, basal ganglia and thalamus. The major model components include single compartment, conductance-based biophysical models of the STN, globus pallidus externa (GPe), globus pallidus interna (GPi) and thalamus, each of which have been validated and employed in previous modelling studies [8]–[10]. The cortex is represented by a network of interneurons and multi-compartment cortical neurons. Each component is described in greater detail below.

Six hundred cells consisting of one hundred STN, GPe, GPi, thalamic, interneuron and cortical neurons were connected through excitatory and inhibitory synapses, AMPA and GABAa, respectively. The STN neurons received direct excitatory input from the cortex via the hyperdirect pathway and inhibitory input from the GPe. Each STN neuron received excitatory input from five cortical neurons and inhibitory input from two GPe neurons. Each GPe neuron received inhibitory input from one other GPe neurons and excitatory input from two STN neurons. Each GPi neuron received excitatory input from a single STN neuron and inhibitory input from a single GPe neuron. Each thalamic neuron received inhibitory input from a single GPi neuron. Cortical neurons received excitatory input from a single thalamic neuron and inhibitory input from a single interneuron. Interneurons received excitatory input from a single cortical axon. All connections within the network were randomly assigned.

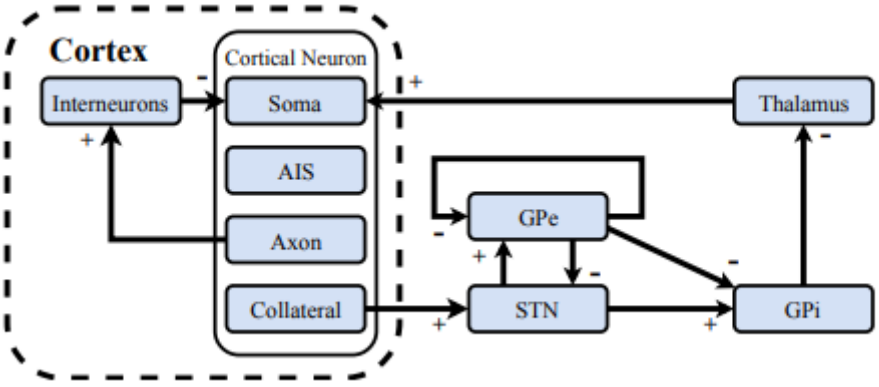

Figure 1: Schematic diagram of the cortico-basal ganglia model. Excitatory and inhibitory connections are indicated with a + or –, respectively.

The presence of pathologically exaggerated beta oscillations in the cortico-basal ganglia network, typically observed in PD, were simulated by varying synaptic gains within the network in accordance with [11]. An increased cortical drive to the STN, due to strengthening of the

hyperdirect pathway, led to the emergence of beta oscillations within the network and the STN LFP.

A. Cortex

The model used to simulate the cortex consisted of cortical neurons and interneurons. The cortical neuron model included a soma, axon initial segment (AIS), main axon, and axon collateral. The cortical neuron soma and interneuron models are based on the regular spiking neuron model developed by Pospischil et al. [12]. The model used to simulate the AIS, main axon, and axon collateral is based on results from the experimental and modeling study in [13]. The membrane potentials of the cortical compartments and interneurons are described by

$$C_m \frac{dv_m}{dt} = -I_l - I_{Na} - I_K - I_{Kd} - I_M - \sum_k I_{syn}^k \quad (1)$$

Where C_m is the membrane capacitance, I_l is the leak current, $I_{N\,a}$ is the sodium current, I_K is the potassium current, I_{Kd} is D potassium current, I_M is a slow, voltage dependent potassium current, and I_{syn} are synaptic currents. The cortical soma model excluded the I_{Kd} current. The cortical AIS, main axon and axon collateral segments did not include the I_M current. Finally, cortical interneurons did not include either the I_{Kd} or I_M currents. Further details regarding the parameters used can be found in [12], [13].

B. Subthalamic Nucleus

The STN model incorporates a physiological representation of STN neurons developed by Otsuka et al. [14]. The model captures the generation of plateau potentials, which are believed to play an important role in generating STN bursting activity in PD. The membrane potential of an STN neuron is given by

$$C_m \frac{dv_m}{dt} = -I_l - I_{Na} - I_K - I_A - I_L - I_T - I_{Ca-K} - \sum_k I_{syn}^k \quad (2)$$

Where C_m is the membrane capacitance, I_l is the leak current, I_{Na} is a sodium current, I_K is a Kv3-type potassium current, I_A is a voltage dependent A-type potassium current, I_L is an L-type long lasting calcium current, $I_{Ca\,K}$ is a calcium activated potassium current, and I_{syn} are synaptic currents. Further details can be found in [14].

C. Globus Pallidus and Thalamus

The models used to simulate GPe, GPi, and thalamic neurons are based on those presented by Rubin and Terman in [15]. The membrane potential of a GP neuron is described by

$$C_m \frac{dv_m}{dt} = -I_l - I_{Na} - I_K - I_T - I_{Ca} - I_{AHP} - \sum_k I_{syn}^k \quad (3)$$

Where C_m is the membrane capacitance, Il is the leak current, I_{Na} is the sodium current, I_K is a potassium current, I_{Na} is a sodium current, I_T is a low-threshold T-type calcium current, I_{Ca} is a voltage-dependent after hyperpolarizaation potassium current, and I_{syn} are synaptic currents. Thalamic neurons were modelled similarly, with the exception of excluding I_{Ca} and I_{AHP} in the thalamic model. Further details regarding the GPe, GPi, and thalamus models can be found in [15].

D. Synapses

Individual synaptic currents, I_{syn}^k, were described by

$$I_{syn}^k = R_k(V_m - E_{rev}) \quad (4)$$

Where I_{syn}^k is the k[th] synaptic current, R_k represents the kinetics of the onset and decay of current following a presynaptic spike for synapse k, and E_{rev} is the reversal potential for the appropriate type of synapse. Further details regarding the synaptic models can be found in [16].

E. Application of DBS and LFP Simulation

The extracellular potential due to a current source, I_x, at time *t* was calculated as

$$V_x(t) = \frac{I_x(t)}{4\pi\sigma r_x} \quad (5)$$

Where σ is the conductivity of a homogenous, isotropic medium representing brain tissue. The distance from a point in extracellular space to the current source I_x, or vice versa, is given as r_x. For simulating the voltage applied to cortical collaterals due to a monopolar stimulation electrode, r_x was the distance between each collateral segment and the stimulation electrode, while I_x was a square wave current source with 130 Hz frequency, 60 s pulse width and varying amplitude. Cortical collaterals were assigned a random position in a 2 mm radius of extracellular space around the stimulation electrode.

To simulate the recording of the LFP using a differential recording electrode, STN neurons, like the cortical collaterals, were assigned positions in a 2 mm radius of extracellular space around the stimulation electrode. Each recording electrode was positioned 1.365 mm away from the stimulation electrode, with each recording electrode being placed either side of the stimulation electrode. The LFP recorded at each recording electrode was then calculated as the summation of the total extracellular voltages due to each STN neuron's synaptic currents in the extracellular space, where I_x corresponds to the synaptic currents of an STN neuron of distance r_x away from one of the recording electrodes.

F. LFP Sample Entropy

Sample Entropy was calculated as the negative natural logarithm of the estimated conditional probability that two sequences similar for *m* points remain similar at the next point, where self-matches are not included in calculating the probability [17]. It is defined as

$$SampEn(m, r, N) = -\ln[A^{m+1}(r)/A^m(r)] \quad (6)$$

Where $A^{m+1}(r)$ represents the number of vector pairs (within the time series) of length $m + 1$ whose mutual distance is less than a tolerance *r*, and $A^m(r)$ equals the number of vector pairs (within the time series) of length *m* whose mutual distance is less than *r*. Here the length of the vector pairs, *m*, denotes the embedding dimension. The mutual distance between the vector pairs was calculated using the Chebyshev distance between the pairs, with *m* and *r* set to 4 and 20% of the standard deviation of the data respectively

G. Firing Pattern Entropy

The firing pattern entropy of a spike train was calculated by binning the inter spike intervals of the train in logarithmic time, as in [18]. The leftmost and rightmost bin edges were set just below, or just above, the smallest and largest inter spike intervals observed, respectively, in each population. The entropy of the spike train was then calculated using Shannon Entropy

$$H(X) = -\sum_{i=0}^{N-1} P_{ISI_i} \log_2(P_{ISI_i}) \qquad (7)$$

Where H is the entropy of spike train X, P_{ISI_i} is the probability of inter spike interval i occurring in the spike train, and N is the number of inter spike interval bins.

H. Simulation Details

The model was implemented in Python using the API package PyNN [19] with NEURON v7.6.5 as the model simulator. A timestep of 0.01 ms was used for simulations. Post-processing was done using custom scripts in MATLAB (The MathWorks, Inc., Natick, MA). To examine LFP sample entropy the LFP was first down-sampled and low-pass filtered at 100Hz to remove stimulation artifact. To examine the magnitude of beta-band oscillations in the LFP the LFP was band-pass filtered between 10 and 35 Hz, full-wave rectified and averaged by low-pass filtering at 2 Hz.

Results

A. LFP Sample Entropy

The effect of varying stimulation amplitude on the STN LFP sample entropy was investigated using a fixed frequency and pulse width of 130 Hz and 60 μs, respectively, Fig. 2 (a). A progressive increase in the sample entropy was observed as the stimulation amplitude increased. For comparison, the corresponding magnitude of beta-band oscillations in the LFP is given in Fig. 2 (b).

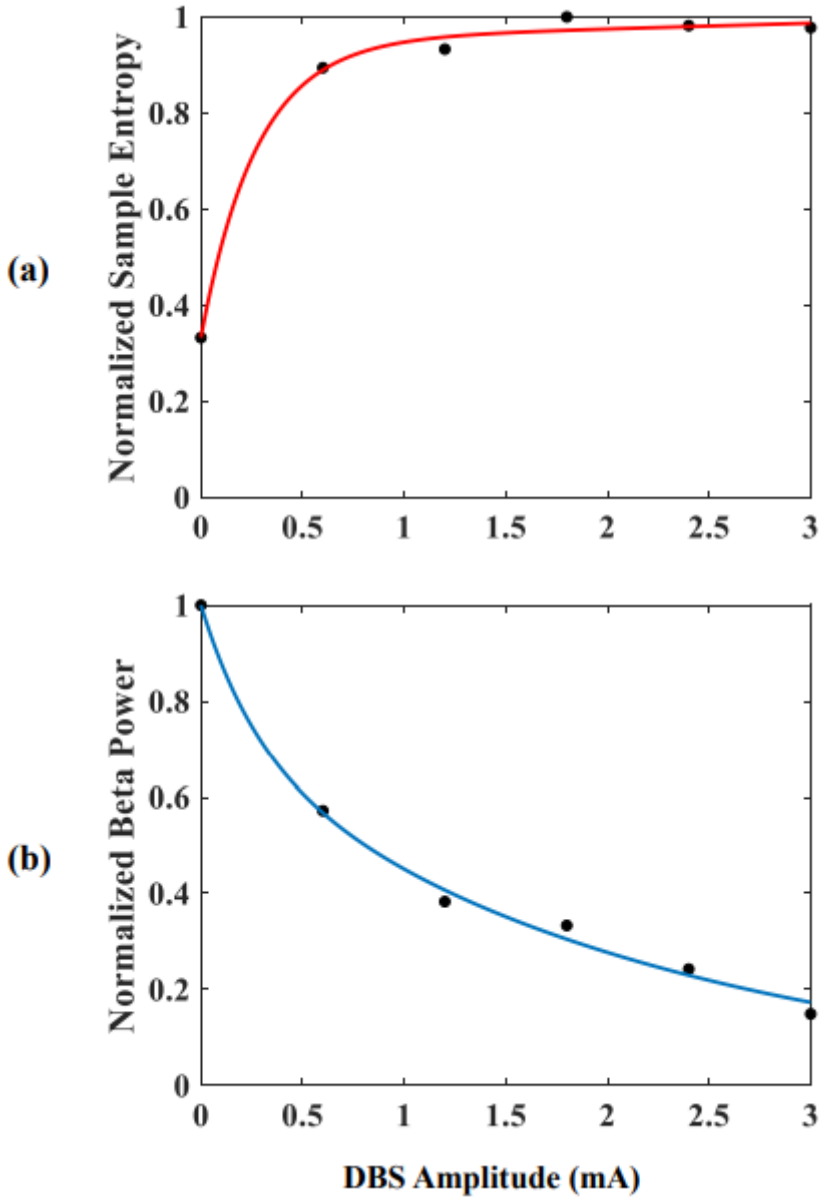

Figure 2. Normalized STN LFP (a) sample entropy and (b) beta-band oscillation power as a function of DBS amplitude.

B. Firing Pattern Entropy

The effect of varying stimulation frequency on the firing pattern entropy of GPe and GPi neurons was investigated using a fixed amplitude and pulse width of 3 mA and 60 μs, respectively. Fig. 3 shows the cumulative distribution of the firing pattern entropy for each population. Firing pattern entropy was reduced following the application of high frequency stimulation (HFS), with a frequency of 130 Hz, and increased following the application of low frequency stimulation (LFS), with a frequency of 20 Hz.

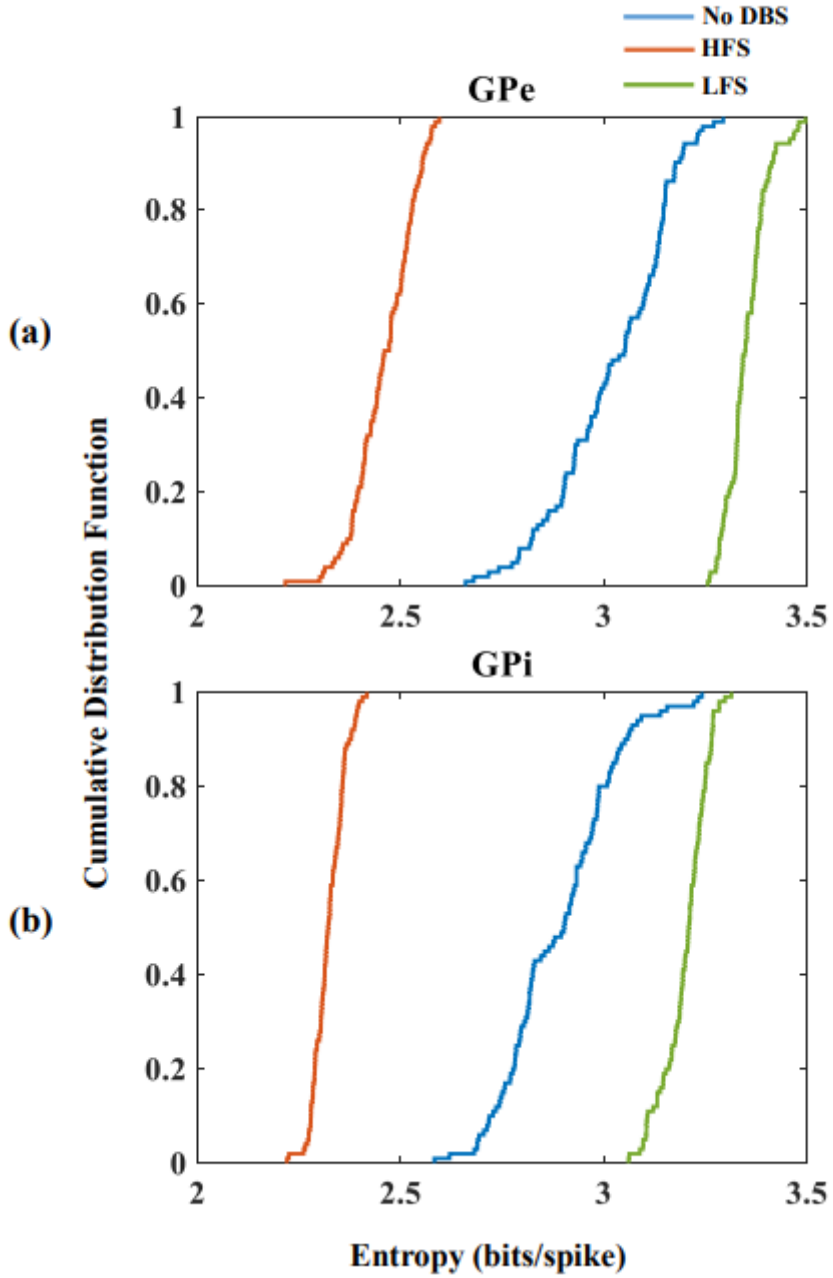

199

200 **Figure 3.** Cumulative distributions of the firing pattern entropy for the (a) GPe and (b) GPi
201 neuron populations due to high frequency and low frequency stimulation.

202 ## Discussion & Conclusion

203 The aim of this study was to investigate changes in neuronal entropy due to extracellular DBS
204 in a computational model of the cortico-basal ganglia network during PD. The model includes
205 extracellular stimulation of cortical afferent fibers projecting to the STN and simulation of the

206 resulting LFP. This allows for comparison with clinical and experimental results which have
207 previously investigated entropy changes in the cortico-basal ganglia network during PD. Sample
208 entropy was observed to have an inverse relationship with beta-band oscillation power, Fig. 2.
209 In [7], an inverse relationship was observed between beta-band sample entropy and beta-band
210 oscillation power taken from STN LFP recordings in freely moving patients during three
211 movement tasks. Here, a distinction was not made between frequency bands when calculating
212 sample entropy. However, effective DBS did result in similar behaviour, with beta-band power
213 decreasing, and sample entropy increasing in the LFP for increasing DBS amplitude.

214 Firing pattern entropy in GP neurons decreased during HFS, and increased during LFS of the
215 STN, Fig. 3. These results agree with those presented in [4]–[6] and support the hypothesis that
216 effective DBS regularizes firing patterns in GP neurons. The computational model presented
217 displays changes in neuronal entropy consistent with those presented in clinical and
218 experimental literature. These results suggest that investigation into basal ganglia entropy
219 changes during PD and DBS may elucidate the relationship between network entropy and
220 oscillation power during disease progression. Moreover, these results support further
221 investigation of the utilization of entropy-based measures in closed-loop DBS strategies.

222

References

[1] A. A. Kuhn, ¨ et al., ”High-Frequency Stimulation of the Subthalamic Nucleus Suppresses Oscillatory β Activity in Patients with Parkinsons Disease in Parallel with Improvement in Motor Performance”, J. Neurosci., vol. 28, no. 24, pp. 6165-6173, Jun. 2008.

[2] C. De Hemptinne, et al., ”Therapeutic deep brain stimulation reduces cortical phase-amplitude coupling in Parkinsons disease”, Nat. Neurosci., vol. 18, no. 5, pp. 779-786, 2015.

[3] A. D. Dorval, A. Muralidharan, A. L. Jensen, K. B. Baker, and J. L. Vitek, ”Information in Pallidal Neurons Increases with Parkinsonian Severity”, Parkinson & Rel. Dis., vol. 21, no. 11, pp. 1355-1361, 2015.

[4] A. D. Dorval, G. S. Russo, T. Hashimoto, W. Xu, W. M. Grill, and J. L. Vitek, ”Deep Brain Stimulation Reduces Neuronal Entropy in the MPTP-Primate Model of Parkinsons Disease”, J. Neurophysiol., vol. 100, no. 5, pp. 2807-2818, 2008.

[5] A. D. Dorval and W. M. Grill, ”Deep brain stimulation of the subthalamic nucleus reestablishes neuronal information transmission in the 6-OHDA rat model of parkinsonism.”, J. Neurophysiol., vol. 111, no. 10, pp. 1949-59, May 2014

[6] A. D. Dorval, A. M. Kuncel, M. J. Birdno, D. A. Turner, and W. M. Grill, ”Deep Brain Stimulation Alleviates Parkinsonian Bradykinesia by Regularizing Pallidal Activity”, J. Neurophysiol., vol. 104, no. 2, pp. 911-921, 2010.

[7] J. Syrkin-Nikolau, et al., ”Subthalamic neural entropy is a feature of freezing of gait in freely moving people with Parkinsons disease”, Neurobiol. Dis., vol. 108, no. June, pp. 288-297, 2017.

[8] E. M. Dunn and M. M. Lowery, ”A model of the cortico-basal ganglia network and local field potential during deep brain stimulation”, 2015 7th Int. IEEE/EMBS Conf. Neural Eng., pp. 848-851, 2015.

[9] G. Kang and M. M. Lowery, ”Interaction of oscillations, and their suppression via deep brain stimulation, in a model of the corticobasal ganglia network”, IEEE Trans. Neural Syst. Rehabil. Eng., vol. 21, no. 2, pp. 244-253, 2013.

[10] G. Kang and M. M. Lowery, ”Effects of antidromic and orthodromic activation of STN afferent axons during DBS in Parkinsons disease: a simulation study”, Front. Comput. Neurosci., vol. 8, no. 32, 2014.

[11] R. J. Moran, et al., ”Alterations in brain connectivity underlying beta oscillations in parkinsonism”, PLoS Comput. Biol., vol. 7, no. 8, 2011.

[12] M. Pospischil, et al., ”Minimal Hodgkin-Huxley type models for different classes of cortical and thalamic neurons”, Biol. Cybern., vol. 99, no. 4-5, pp. 427-441, Nov. 2008.

[13] A. J. Foust, Y. Yu, M. Popovic, D. Zecevic, and D. A. Mccormick, ”Somatic Membrane Potential and Kv1 Channels Control Spike Repolarization in Cortical Axon Collaterals and Presynaptic Boutons”, vol. 31, no. 43, pp. 15490-15498, 2011.

[14] T. Otsuka, T. Abe, T. Tsukagawa, and W. J. Song, ”Conductance-Based Model of the Voltage-Dependent Generation of a Plateau Potential in Subthalamic Neurons”, J. Neurophys., vol. 92, no. 1, 2004.

[15] J. E. Rubin and D. Terman, ”High Frequency Stimulation of the Subthalamic Nucleus Eliminates Pathological Thalamic Rhythmicity in a Computational Model”, J. Comput. Neurosci., vol. 16, no. 3, pp. 211-235, 2004.

[16] A. Destexhe, Z. F. Mainen, and T. J. Sejnowski, ”An Efficient Method for Computing Synaptic Conductances Based on a Kinetic Model of Receptor Binding”, Neural Comp., vol. 6, pp. 14–18, 1994.

[17] J. S. Richman and J. R. Moorman, ”Physiological time-series analysis using approximate entropy and sample entropy”, Am. J. Physiol. Circ. Physiol., vol. 278, no. 6, pp. H2039-H2049, 2000.

[18] A. D. Dorval, ”Probability Distributions of the Logarithm of Inter–Spike Intervals yield Accurate Entropy Estimates from Small Datasets”, J. Neurosci. Methods, vol. 173, no. 1, pp. 129-139, 2009.

[19] A. P. Davison, ”PyNN: a common interface for neuronal network simulators”, Front. Neuroinform., vol. 2, no. January, pp. 1-10, 2008.

276